

# Effect of DC Link Capacitor on the Performance of Wind-Driven Double-Fed Induction Generator

SANAA M I AMER, MONA N ESKANDER  
Department of Power Electronics and Energy Conversion,  
Electronics Research Institute,  
Cairo,  
EGYPT

*Abstract:* - In this paper, the starting performance of a double-fed induction generator (DFIG) operating at super-synchronous speed is investigated when varying the values of the DC link capacitor. The starting transients, the settling time, and the harmonics of the stator and rotor currents and voltages are investigated as a function of the DC link capacitor  $C_d$ . Curve fitting is applied to derive mathematical equations (polynomial) relating the variation of the stator current THD with the value of the DC capacitor. Similarly, polynomials are deduced to relate the THD of the rotor current and rotor voltage with the value of the DC link capacitor. These polynomials help to design the DC link parameters that lead to minimum current and voltage harmonics of the grid-connected DFIG. The minimum THD values of the stator current, rotor current, and rotor voltage are presented. These results are repeated at different rotor speeds to deduce the optimum  $C_d$  value within a wide speed range. Also, the effect of  $C_d$  on the DC link current and voltage ripples is demonstrated at different speeds.

*Key-Words:* - double-fed induction generator, super-synchronous speed, DC link capacitor, THD, DC ripples, starting transients, settling time, stator harmonics, rotor harmonics.

Received: February 25, 2023. Revised: December 11, 2023. Accepted: December 21, 2023. Published: March 12, 2024.

## 1 Introduction

Power generation from wind energy, as a renewable non-polluting energy source, is preferably done with DFIG (Doubly Fed Induction Generator) due to the low ratings of the rotor converters leading to an economic generation system, [1], [2], [3], [4], [5]. The rotor of the DFIG is mechanically coupled to the wind turbine, while the stator windings of the DFIG are directly connected to the grid. The rotor windings are connected to the grid via slip rings and an AC/DC/AC converter (rectifier and inverter with a common DC link). The maximum power that the rotor converters of the DFIG have to handle under steady-state conditions is a fraction of the DFIG machine-rated power. This fraction is approximately equal to the 30% of the rated power, [6].

Recent studies showed that faults in the power electronic converters account for a great share of the overall wind turbine systems faults, [7], [8], [9]. The DC link capacitors are regarded as one of the weakest parts in back-to-back power converters, [10], [11]. The DC link capacitor ripple current causes thermal stress, leading to a high percentage of the overall capacitor losses, [12]. Hence, it is

clear that the DC link capacitor impacts the performance of the DFIG, not only during its steady state operation but also at starting and during grid voltage fluctuations. It also affects the total harmonic distortion THD of the DFIG voltages and currents. Hence the DC link filter must be carefully designed to attain optimum DFIG performance at starting, at steady state, and during grid voltage sags and swells.

In this paper, the effect of the DC link capacitor on the starting transients, the settling time, and the harmonics of the stator and rotor currents, and stator and rotor voltages, are being investigated. Moreover, the DC voltage and current ripples are calculated at different values of  $C_d$ . The THD of the stator current, the rotor current, and rotor voltage at different values of the DC capacitor; are also deduced. Mathematical equations relating the variation of the stator current, rotor current, and rotor voltage THD with the value of the DC capacitor are deduced. These results help in designing the DC link filter components to attain minimum transients' settling time and minimum harmonics for better performance of the DFIG. The

ripples of the DC link voltage and current are deduced and plotted versus Cd.

The contribution achieved in this paper can be summarized as follows:

i. demonstrating the effect of the DC link capacitor on the magnitude of starting current and voltage transients and on their settling time, which leads to safe starting

ii. deducing mathematical equations to relate the value of the DC link capacitor with the harmonics of stator current and rotor voltage and rotor current, which helps in designing the DC link components to minimize the current and voltage harmonics.

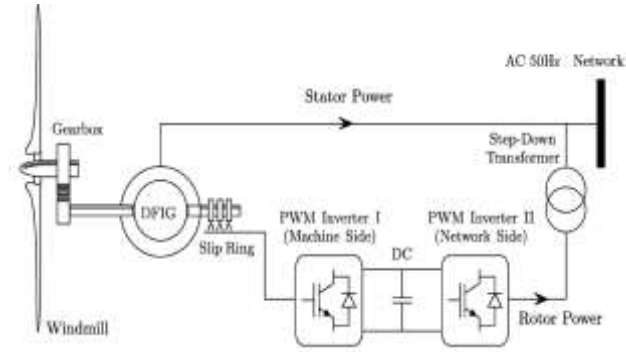


Fig. 1: The DFIG with back-to-back converters

## 2 Mathematical model of DFIG

Figure 1 shows the configuration of the DFIG with back-to-back converters and the DC link. The DFIG dynamic equations in the d-q synchronously rotating frame are given as, [13]:

$$\frac{d\lambda_{ds}}{dt} = v_{ds} - r_s i_{ds} + w\lambda_{qs} \quad (1)$$

$$\frac{d\lambda_{qs}}{dt} = v_{qs} - r_s i_{qs} + w\lambda_{ds} \quad (2)$$

$$\frac{d\lambda_{dr}}{dt} = v_{dr} - r_r i_{dr} + (w-w_r)\lambda_{qr} \quad (3)$$

$$\frac{d\lambda_{qr}}{dt} = v_{qr} - r_r i_{qr} - (w-w_r)\lambda_{dr} \quad (4)$$

$$\frac{dw_r}{dt} = \frac{1}{2H} (T_e - T_L - B_m w_r) \quad (5)$$

$$\lambda_{ds} = L_s i_{ds} + L_m i_{dr} \quad (6)$$

$$\lambda_{qs} = L_s i_{qs} + L_m i_{qr} \quad (7)$$

$$\lambda_{dr} = L_r i_{dr} + L_m i_{ds} \quad (8)$$

$$\lambda_{qr} = L_r i_{qr} + L_m i_{qs} \quad (9)$$

The electric torque equation is:

$$T_e = \frac{3PL_m}{2L_s} (\lambda_{qs} i_{dr} - \lambda_{ds} i_{qr}) \quad (10)$$

Where,  $\lambda$ ,  $v$ ,  $i$ ,  $\omega$ ,  $T_e$  denote flux, voltage, current, angular speed, and electromagnetic torque respectively. Suffixes d and q denote the d-axis component and q-axis component in the synchronously rotating d-q reference frame, respectively.  $r$  and  $L$  denote resistance and inductance, respectively. Suffixes s, r, and m denote stator, rotor, and mutual parameters respectively;  $P$  is the number of pole pairs

The power balance equation in the DC link, [14]:

$$P_{in} = P_{out} + C_{dc} V_{dc} \frac{dV_{dc}}{dt} \quad (11)$$

$$P_{bus} = P_{in} - P_{out} - P_l \quad (12)$$

Where  $P_{in}$  is power given by inverter I, shown in Figure 1,  $P_{out}$  is power output from DC link,  $P_l$  is DC link losses.

Substituting equation (11) in equation (12) gives:

$$P_{bus} = C_{dc} V_{dc} \frac{dV_{dc}}{dt} \quad (13)$$

$$P_{bus} = \frac{dW_{bus}}{dt} \quad (14)$$

$$W_{bus} = \frac{1}{2} C_{dc} V_{dc}^2 \quad (15)$$

Where  $V_{dc}$  is the instantaneous voltage and  $W_{bus}$  is the instantaneous energy stored in a capacitor.

## 3 Results and Discussion

Equations (1-15) describing the grid-connected DFIG at starting and during steady-state operation are simulated using Matlab/Simulink software. The system performance is investigated at two super-synchronous speeds namely; 1850 rpm and 1900 rpm. The DC capacitor is varied at each speed to study its influence on the DFIG performance. The following results are obtained.

### 3.1 The Settling Time after Starting

Figure 2 shows the profiles of the stator voltage, stator current, rotor voltage, and rotor current at starting when the reference speed is 1850 rpm with  $C_d=0.025F$ . Figure 3, Figure 4 and Figure 5 show the starting profiles at  $C_d= 0.01F$ ,  $C_d=.0075F$ , and  $C_d=0.005F$  respectively. It is worth noticing that the stator voltage is not affected by  $C_d$ . These results

clarify the effect of the dc link capacitor on the settling time, showing the decrease in starting transients settling time with the increase in value of Cd. It is noted that the magnitudes of the currents and voltages starting transients are nearly equal, i.e. not affected by the dc link capacitor.

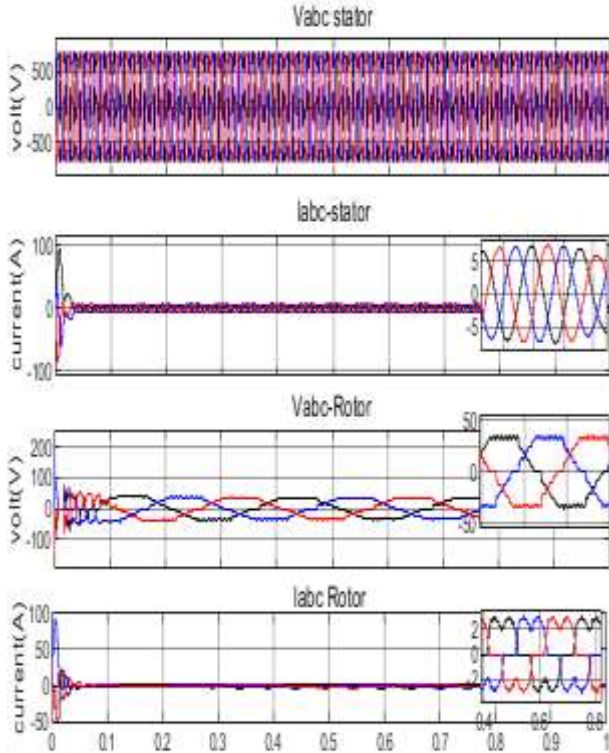


Fig. 2: Voltage and current profiles at Cd=0.025F, 1850 rpm

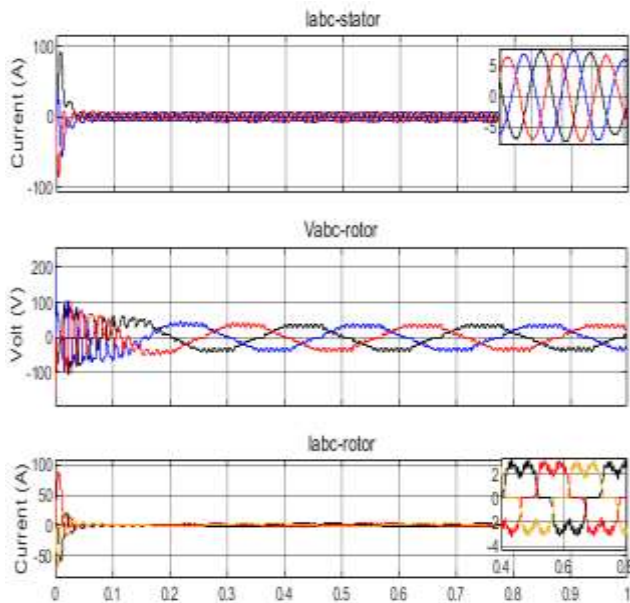


Fig. 3: Voltage and current profiles at Cd=0.01F, 1850 rpm

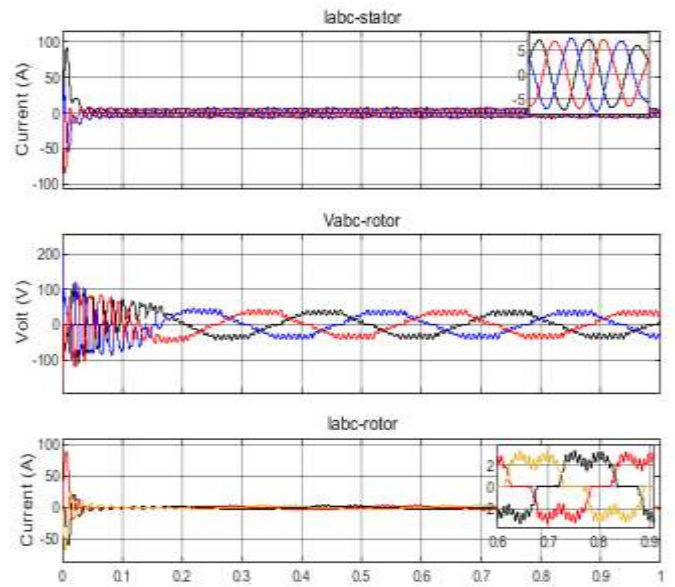


Fig. 4: Voltage and current profiles at Cd=.0075F, 1850 rpm

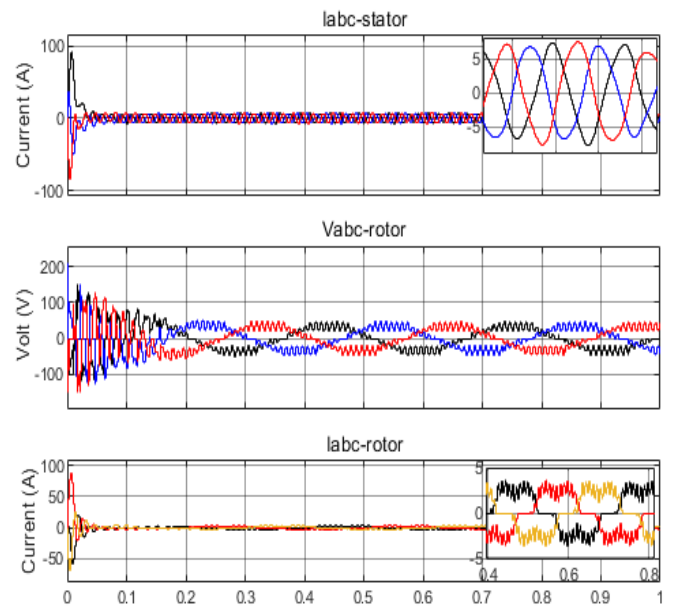


Fig. 5: Voltage and current profiles at Cd=.005F, 1850 rpm

To prove the effect of Cd on starting transients, the stator current, the rotor current, and the rotor voltage at starting are calculated with the same values of the DC link capacitor at 1900 rpm reference speed. Figure 6, Figure 7, Figure 8 and Figure 9 show the stator current, rotor voltage, and rotor current at Cd=0.025F, 0.01F, 0.0075F, and 0.005F respectively.

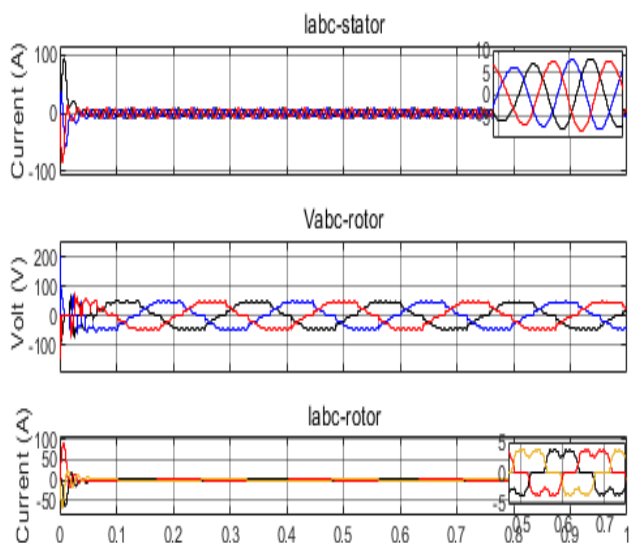


Fig. 6: Voltage and current profiles at  $C_d=0.025F$ , 1900 rpm

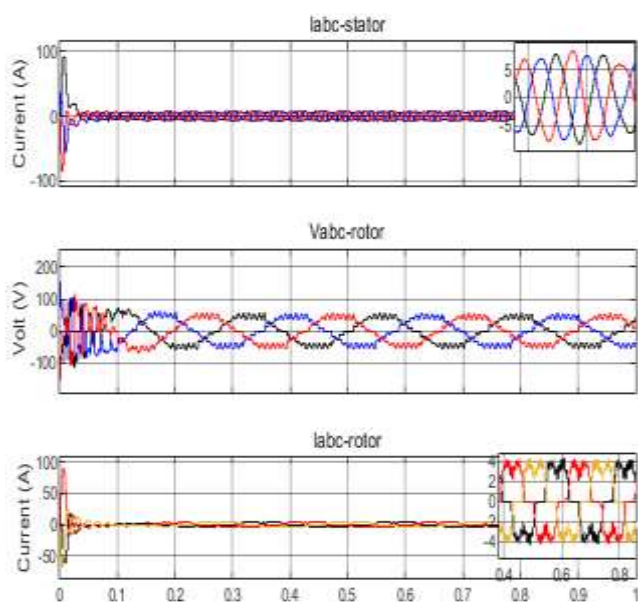


Fig. 7: voltage and current profiles at  $C_d=0.01F$ , 1900 rpm

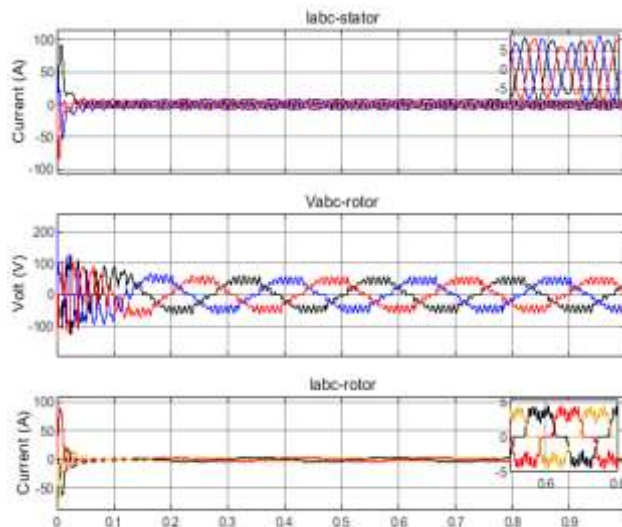


Fig. 8: Voltage and current profiles at  $C_d=0.0075F$ , 1900 rpm

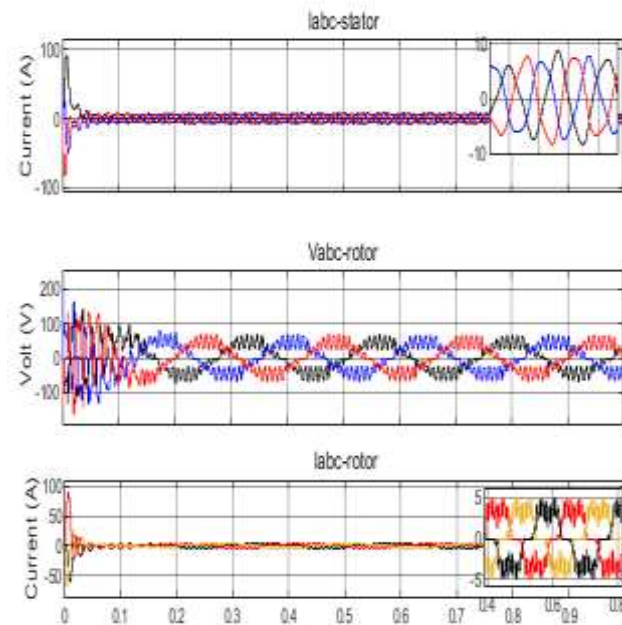


Fig. 9: voltage and current profiles at  $C_d=.005F$ , 1900 rpm

From these figures, it is clear that the settling times of the stator and rotor currents and rotor voltage are affected by  $C_d$  value while the magnitude of these transients are not affected. To clarify the effect of  $C_d$  on the starting transient settling time, the settling time ( $t_s$ ) is plotted as a function of the DC link capacitor as shown in Figure 10. The starting transient settling time decreases drastically as  $C_d$  increases, revealing the influence

of the dc link capacitor on the stator as well as on the rotor currents and voltages.

It is noted from Figures 2, Figure 3, Figure 4, Figure 5, Figure 6, Figure 7, Figure 8 and Figure 9 that settling time  $t_s$  differs for each variable, i.e.  $t_s$  of stator current lower than  $t_s$  of rotor current. In Figure 10, the longest  $t_s$  (that of  $i_r$ ) is plotted versus  $C_d$ . An exponential decrease in the settling time occurs as  $C_d$  increases.

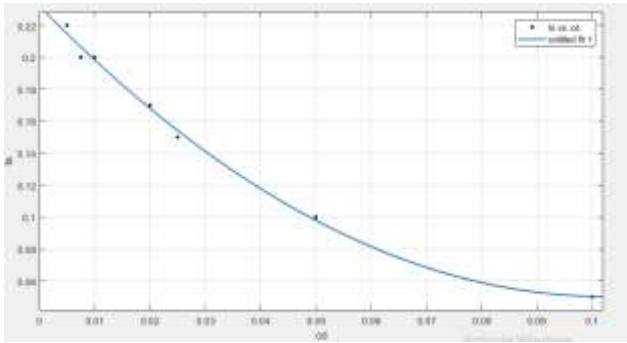


Fig. 10: Variation of rotor current starting transient settling time with DC link capacitor

### 3.2 Effect of $C_d$ on Current and Voltage Harmonics

Suppressing current harmonics is essential for the grid-tied doubly-fed induction generator (DFIG) to prevent grid distortion, especially in weak grids or grids with a large number of connected wind energy sources. Sources of DFIG harmonics include switching of the two back-to-back rotor converters, as well as wind speed fluctuations. In this section, the variation of currents' and voltages' harmonics (THD) with  $C_d$  is investigated and the results are plotted. These results are then interpolated in the form of mathematical equations relating the THD of each variable with the value of  $C_d$ . These equations help in determining the dc link capacitor value to minimize the harmonics of each variable.

#### 3.2.1 Variation of Stator Current Harmonics with $C_d$

In Figure 11, the THD of the stator current is plotted versus  $C_d$  showing minimum harmonics distortion at  $C_d = 0.01F$ .

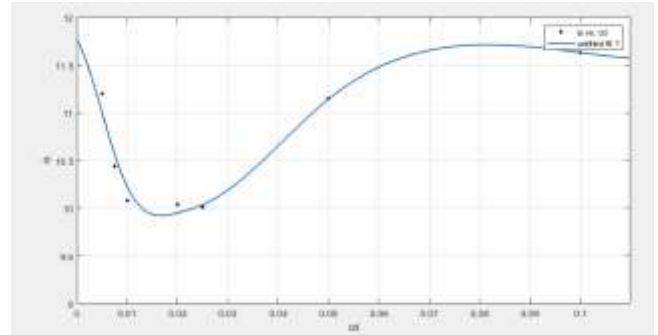


Fig. 11: Variation of stator current THD with Dc link capacitor

Interpolating the THD versus  $C_d$  curve led to the following polynomial.

General model:

$$f(x) = (p1 * x^2 + p2 * x + p3)/(x^4 + q1 * x^3 + q2 * x^2 + q3 * x + q4) \quad (16)$$

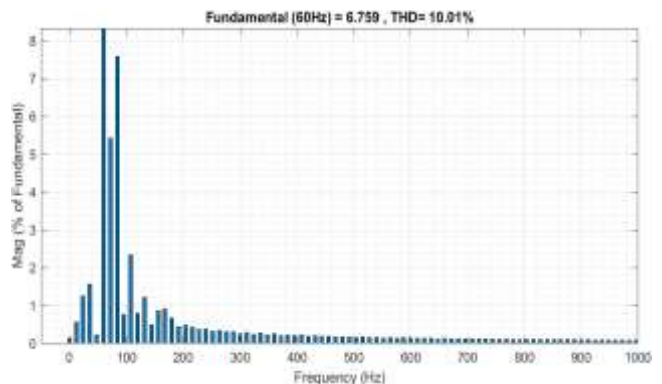
where  $x$  stands for  $C_d$  and the coefficients are given by:

$$p1 = 2.675e^4 \quad p2 = 3e^4 \quad p3 = 3.086e^4 \\ q1 = 215.2 \quad q2 = 1854 \quad q3 = 2423 \quad q4 = 3020$$

Goodness of fit:

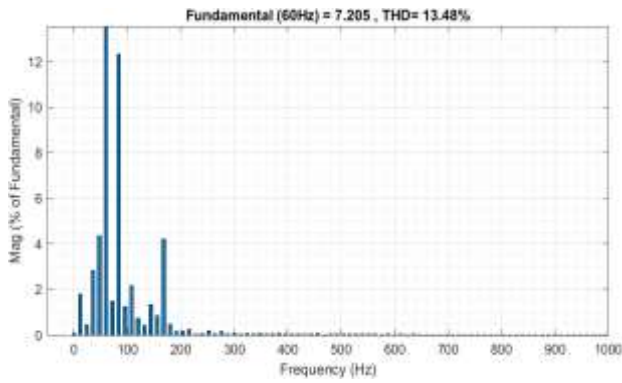
SSE (sum squared error): 0.1952

Figures 12a and 12b show the minimum THD of the stator current. A 10.01% THD occurred at  $C_d = 0.01F$  for both reference speeds: 1850 rpm and 1900 rpm.



(a) at 1850 rpm





(b) at 1900 rpm

Fig. 12: Stator current THD

### 3.2.2 Variation of Rotor Current Harmonics with Cd

In Figure 13, the THD of the rotor current is plotted versus Cd showing minimum harmonics distortion at Cd= 0.005F.

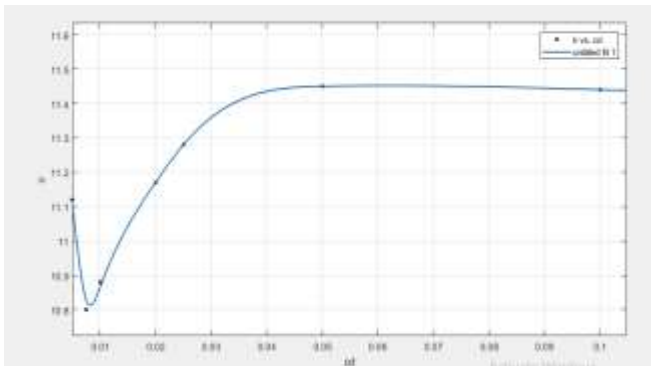


Fig. 13: Variation of rotor current THD with DC link capacitor at 1850 rpm

### 3.2.3 Variation of Rotor Voltage Harmonics with Cd

In Figure 14, the THD of the rotor voltage is plotted versus Cd showing minimum harmonics distortion at Cd= 0.065F

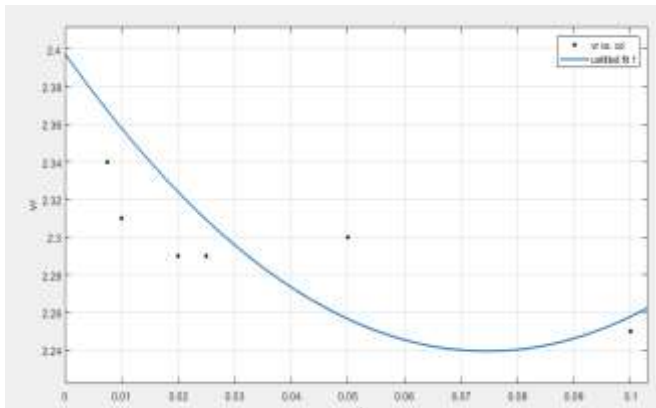


Fig. 14: Variation of rotor voltage THD with Cd at 1850 rpm

Applying curve fitting to the plotted rotor voltage versus Cd shown in Figure 14, the following polynomial is deduced:

$$f(x) = p1 * x^2 + p2 * x + p3 \quad (17)$$

where x stands for Cd and the calculated coefficients are given by:

$$p1 = 28.43 (-51.4, 109.3)$$

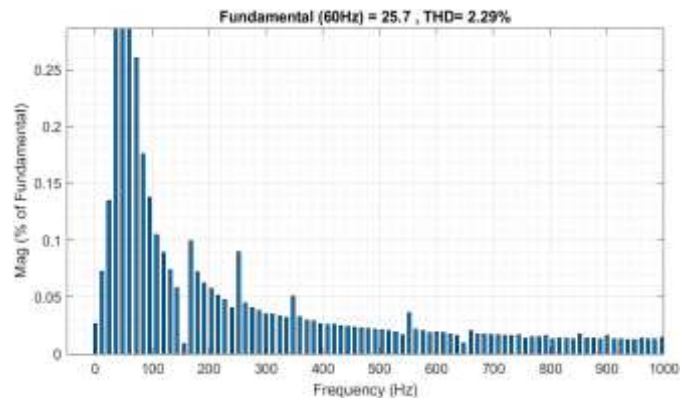
$$p2 = -4.239(-12.9, 4.433)$$

$$p3 = 2.397(2.26, 2.535)$$

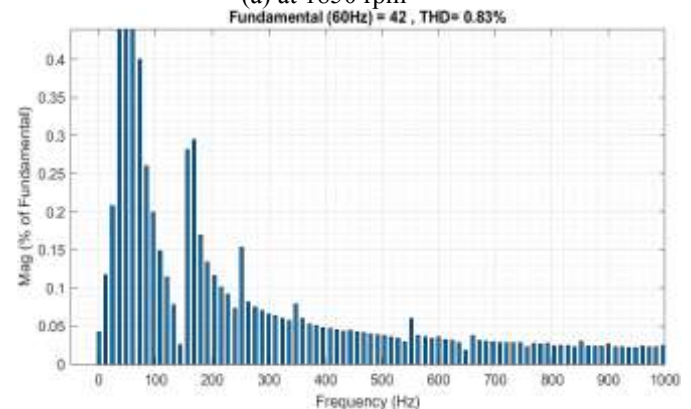
Goodness of fit:

SSE (sum squared error): 0.01517

The minimum value of the rotor voltage THD at 1850 rpm is 2.29%, occurred at Cd=0.065F, as shown in Figure 15a. The minimum value of the rotor voltage THD at 1900 rpm is 0.83%, occurred at Cd=0.01F, as shown in Figure 15b. These results help to choose a value for Cd according to the operating speed range, since Cd for minimum THD differs according to the speed.



(a) at 1850 rpm



(b) at 1900 rpm

Fig. 15: Minimum THD of rotor voltage

### 3.3 Effect of DC Link Capacitor on DC Voltage Ripple

Ripple is wasted power, and has many undesirable effects on the DC circuit. It heats its components, causes noise and distortion. The DC-link capacitor is the most vulnerable component of a voltage conversion system. It is responsible approximately for 30% of failures in power converters, [11]. The current flowing through the capacitor causes power loss over the effective series resistance (ESR), leading to temperature rise, which results in shortening the life span of the capacitor, [12]. In back to back converters system, the DC-link capacitor is subjected to constant stress, since it handles the current, flowing through it from the rectifier and the inverter sides, [13]. To prolong the lifespan of the Cd, connecting more capacitors in parallel to share the ripple current was suggested. This approach is effective in terms of failure prevention. However, it increases the size and the cost of the system, [14]. Hence studying the DC current and DC voltage ripples as a function of the DC link capacitor is essential for the safety of power electronics components.

Also comparing the value of Cd giving minimum DC ripples with the Cd value (given in the last section) resulting in minimum THD, enables the choice of the DC link capacitor for optimal operation of the DFIG.

Figure 16, Figure 17, Figure18 and Figure 19 demonstrate the DC link voltage and current at 1850 rpm and Cd=0.025 F, 0.01F, 0.0075F, and 0.005 respectively. As expected, the ripples of voltage and current increase as Cd decreases. To study the level of DC ripples at higher speeds, Figure 20, Figure 21, Figure 22 and Figure 23 demonstrate the DC link voltage and current at 1900 rpm and Cd=0.025F, 0.01F, 0.0075F, and 0.005 respectively. Higher ripples occurred at higher DFIG speed.

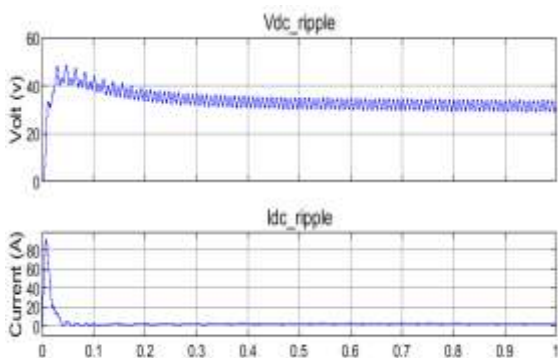


Fig. 16: DC link voltage and current at 1850 rpm & Cd=0.025 F

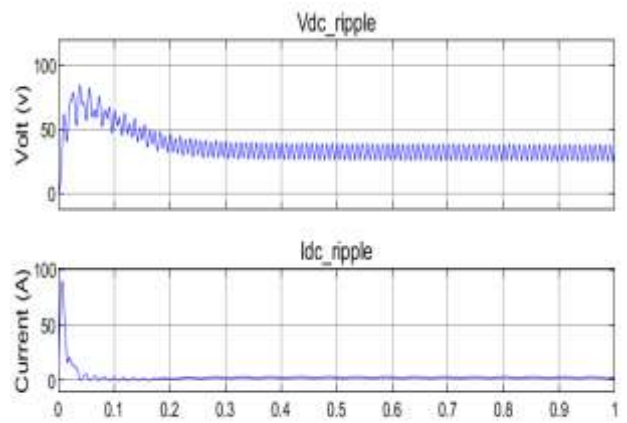


Fig. 17: DC link voltage and current at 1850 rpm & Cd=0.01 F

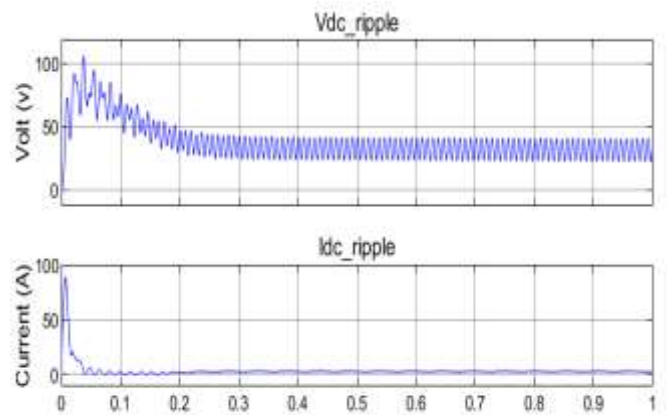


Fig. 18: DC link voltage and current at 1850 rpm & Cd=0.0075 F

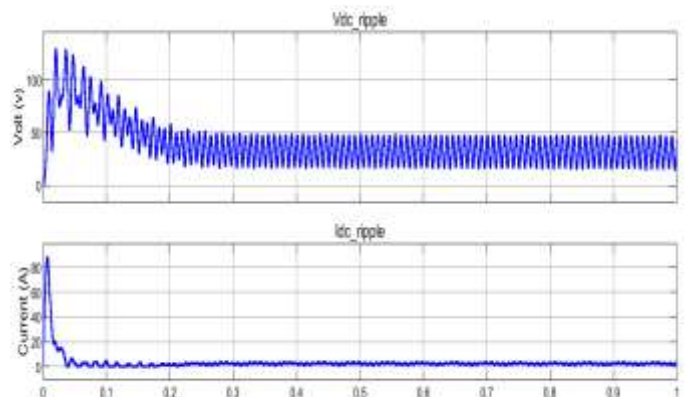


Fig. 19: DC link voltage and current at 1850 rpm & Cd=0.005 F

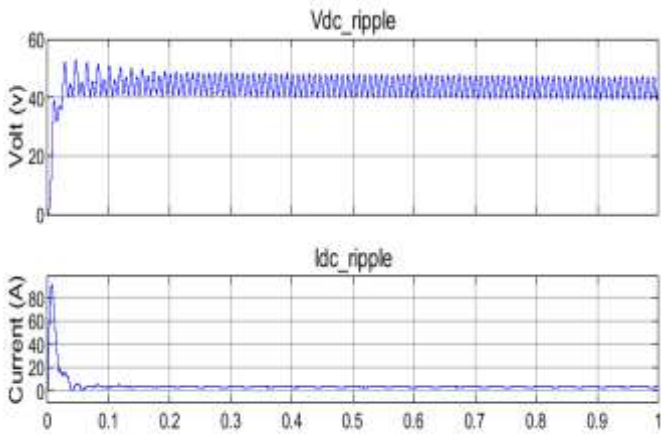


Fig. 20: DC link voltage and current at 1900 rpm & Cd=0.025 F

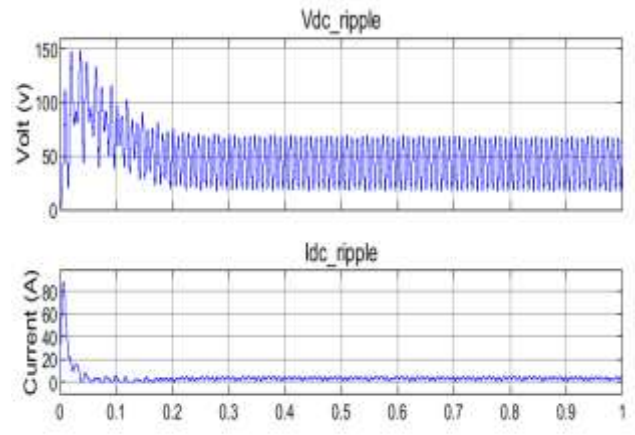


Fig. 23: DC link voltage and current at 1900 rpm & Cd=0.005 F

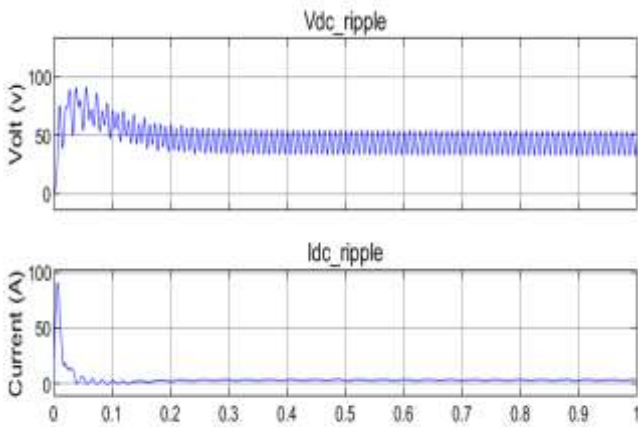


Fig. 21: DC link voltage and current at 1850 rpm & Cd=0.01 F

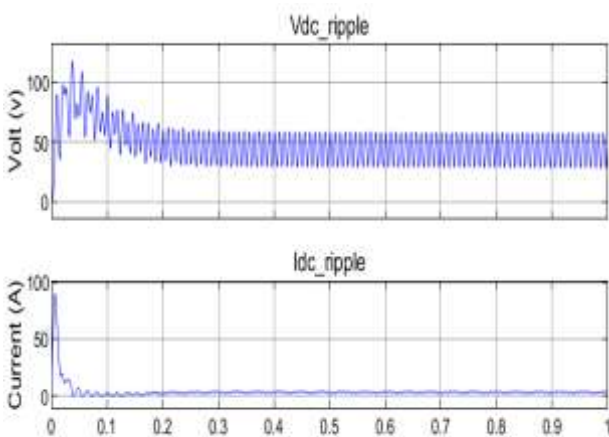


Fig. 22: DC link voltage and current at 1850 rpm & Cd=0.0075 F

The DC link voltage ripple is plotted versus Cd in Figure 24 and Figure 25 at 1850 rpm and 1900 rpm respectively. These plots prove the increase in voltage ripple as speed increases. It also shows an exponential decrease in voltage ripple with an increase in Cd.

Similarly, Figure 26 and Figure 27 prove the increase in DC link current ripples as the speed increases from 1850 rpm to 1900 rpm. These plots demonstrate the fast decrease in current ripples as Cd increases.

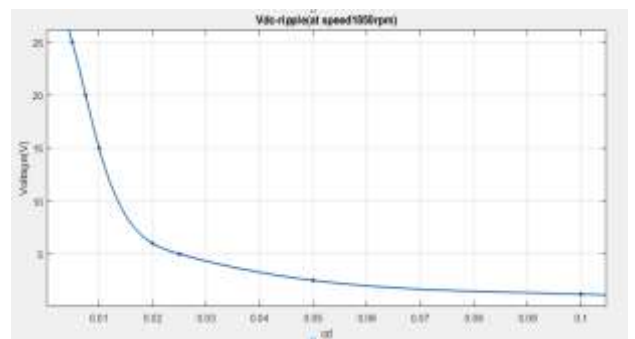


Fig. 24: DC link voltage ripples versus and current Cd at 1850 rpm

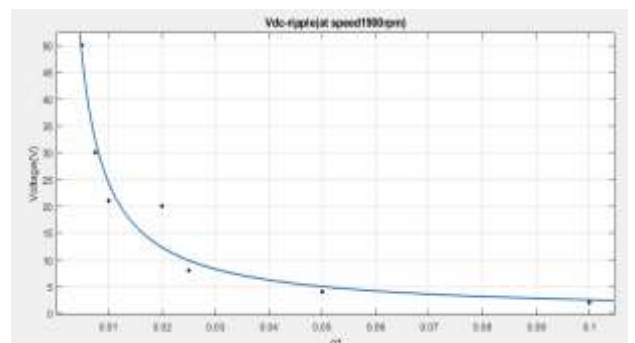


Fig. 25: DC link voltage ripples versus and current Cd at 1900 rpm



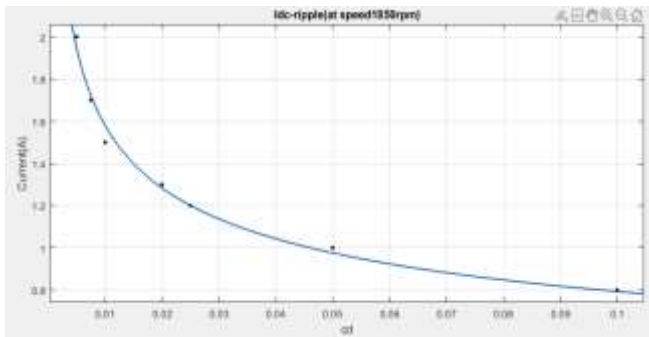


Fig. 26: DC link current ripples versus and current Cd at 1850 rpm

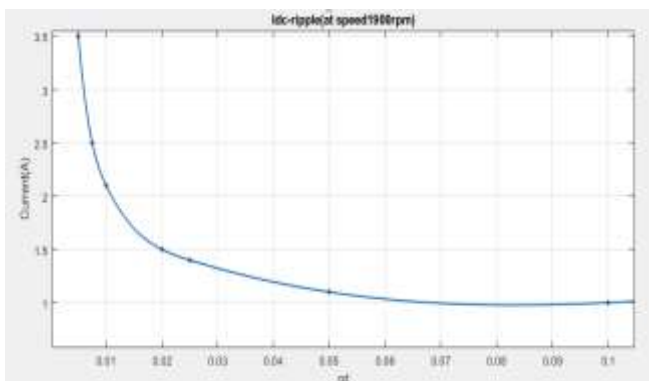


Fig. 27: DC link current ripples versus and current Cd at 1900 rpm

## 4 Applications

The results obtained from the simulations can be applied to design the AC/DC/AC converter interfacing a generator or an electrical drive with the grid to minimize the harmonics injected into the grid. Also, the starting current and voltage transients can be reduced by using a DC link capacitor at starting different from the DC link capacitor during steady state operation. Hence it is clear that Cd affects the power quality of the DFIG, [15].

The DC link capacitor affects greatly the fault ride-through and fault recovery for grid-connected generators or motors, [16].

## 5 Conclusion

The starting voltage and current transients of a double-fed induction generator (DFIG) operating at super-synchronous speed are investigated when varying the values of the DC link capacitor (Cd). The stator current, rotor current, and rotor voltage harmonics are also calculated as Cd is varied. These variables are calculated at two super-synchronous speeds.

The starting transients settling time and the harmonics of the stator current, rotor current, and rotor voltage are highly affected by the value of the DC link capacitance. However, the magnitude of the starting current and starting voltage transients are not affected by Cd.

The value of the DC link capacitor (Cd) that results in minimum stator current harmonics is deduced. Also, the values of Cd that lead to minimum rotor current harmonics and minimum rotor voltage harmonics are deduced. Mathematical equations relating the minimum THD of these variables with Cd are deduced. These equations aid in designing the DC link variables that minimize THD. The results proved that the DC link capacitor resulting in minimum stator current harmonics differs from Cd which led to minimum rotor current harmonics, and Cd which led to minimum rotor voltage harmonics. Since the stator is directly connected to the grid, it is recommended to employ the DC link capacitance that results in minimum stator current harmonics, to avoid grid voltage distortion.

Also, the influence of Cd on the DC link voltage and current ripples is investigated. Results prove that the DC link voltage and current ripples are smoothed as Cd increases.

Future work will focus on the role of Cd during symmetrical and unsymmetrical grid faults and its influence on the fault recovery time.

## References:

- [1] A. Rashad Mohammed Quena, A. M. Hemeida, Mountasser M. M. Mahmoud, "Study and Control of the Dynamic Performance of Grid Connected Doubly Fed Induction Generator Driven by Wind Energy", *International Journal of Applied Energy Systems*, Vol. 1, No. 2, July 2019, pp53-63.
- [2] Shrabani Sahu and Sasmita Behera, "A review on modern control applications in wind energy conversion system", *Energy & Environment journal*, 33(2), February 2021, DOI: 10.1177/0958305X2199592.
- [3] Hamid Chojaa, Aziz Derouich, Mohammed Taoussi, Seif Eddine Chehaidia, Othmane Zamzoum, Mohamed I. Mosaad, Ayman Alhejji, and Mourad Yesséf, "Nonlinear Control Strategies for Enhancing the Performance of DFIG-Based WECS under a

- Real Wind Profile", *Energies* 2022, 15, 6650, pp.1-23, <https://doi.org/10.3390/en15186650>.
- [4] Ola Hussein Abd Ali Alzubaidi, Aya Qusay, "Design and Simulation of Wind Farm Model Using Doubly-Fed Induction Generator Techniques", *Proceedings of International Conference on Emerging Technologies and Intelligent Systems*, January 2022, DOI: 10.1007/978-3-030-82616-1\_7.
- [5] Hamdan1, Marwa M. M. Youssef 1, Omar Noureldeen, "A Review of Intelligent Control Systems for Grid Tie Doubly Fed Induction Generator Based Wind Farm", *International Journal of Engineering Sciences and Applications* (2023), 4(2): 269-278, DOI: 10.21608/svusr.2023.215683.1132.
- [6] Mahmoud A. Saleh, and Mona N. Eskander, "Sizing of Converters Interfacing the Rotor of Wind Driven DFIG to the Power Grid", *Journal of Smart Grid and Renewable Energy*, Vol. 2, No. 3, August 2011.
- [7] H. Jedtberg, M. Langwasser, R. Zhu, G. Buticchi and M. Liserre, "Impacts of rotor current control targets on DC-link capacitor lifetime in DFIG-based wind turbine during grid voltage unbalance," *IEEE Energy Conversion Congress and Exposition (ECCE)*, Cincinnati, OH, 2017, pp. 3489-3495.
- [8] H. Nian, Y. Xu, L. Chen and M. Zhu, "Modeling and Analysis of DC-Link Dynamics in DFIG System with an Indicator Function," *IEEE Access*, vol. 7, pp. 125401-125412, 2019, DOI: 10.1109/ACCESS.2019.2938796.
- [9] I. Ngom, S. Skander, Mustapha, I. Slama Belkhodja, A. Mboup, L. Thiaw, "An Adaptive DC-link Voltage Control for Doubly Fed Induction Generator Wind Turbine System", *2018 International Conference on Electrical Sciences and Technologies in Maghreb (CISTEM)*, <https://doi.org/10.1109/CISTEM44123.2018>.
- [10] H. Wang and F. Blaabjerg, "Reliability of capacitors for dc-link applications in power electronic converters-an overview," *IEEE Trans. Ind. Appl.*, vol. 50, no. 5, pp. 3569-3578, Sept. 2014.
- [11] Arif Sharafat Ali, Khawaja Khalid Mehmood, Ji-Soo Kim, Chul-Hwan Kim, "ESD-based Crowbar for Mitigating DC-link Variations in a DFIG-based WECS", *International Conference on Power Systems Transients (IPST2019) in Perpignan, France June 17-20, 2019*.
- [12] Delmonte, N., Cabezuelo, D., Kortabarria, I., Santoro, D., Toscani, A., and Cova, P, " A method to extract lumped thermal networks of capacitors for reliability oriented design ". *Microelectron. Reliab.* 114, 113737. DOI: 10.1016/j.microrel.2020.113737.
- [13] Kenneth E. Okedu, "Improved Performance of Doubly-Fed Induction Generator Wind Turbine During Transient State Considering Supercapacitor Control Strategy", *Electrica*, 2022; 22(2): 198-210.
- [14] Rekha Parashar, Shashikant, Apoorva Srivastava, "DC Link Capacitor Voltage Stabilization of DFIG under various Fault Conditions", *International Journal of Advance Engineering and Research Development*, Vol. 2, Issue 4, April -2015
- [15] X. Liang, "Emerging Power Quality Challenges Due to Integration of Renewable Energy Sources" *IEEE Trans. Ind. Appl.*, vol. 53, no. 2, pp 855-866, Mar.-Apr. 2017.
- [16] Juan Wei, , Qiuwei Wu, Bin Zhou, Da Xu, Sheng Huang, " MPC-based DC-link voltage control for enhanced high-voltage ride-through of offshore DFIG wind turbine", *International Journal of Electrical Power & Energy Systems*, Vol. 126, Part A, March 2021, 106591.

#### **Contribution of Individual Authors to the Creation of a Scientific Article (Ghostwriting Policy)**

The authors equally contributed in the present research, at all stages from the formulation of the problem to the final findings and solution.

#### **Sources of Funding for Research Presented in a Scientific Article or Scientific Article Itself**

No funding was received for conducting this study.

#### **Conflict of Interest**

The authors have no conflicts of interest to declare.

#### **Creative Commons Attribution License 4.0 (Attribution 4.0 International, CC BY 4.0)**

This article is published under the terms of the Creative Commons Attribution License 4.0

[https://creativecommons.org/licenses/by/4.0/deed.en\\_US](https://creativecommons.org/licenses/by/4.0/deed.en_US)